

Journal of Molecular Science

www.jmolecularsci.com

ISSN:1000-9035

Design, Synthesis and Anticancer Activity of Some Benzimidazole Derivatives

Trivedi Vipul V.¹, Shinde Kiran K.², Shah Darshan V.³, Hapse Sandip A.⁴¹Research Scholar, Shubham University, Bhopal, Madhya Pradesh (MP)-462038²Associate Professor, Vidya Niketan Institute of Pharmacy and Research Center, Bota. Maharashtra (MS)-422602³Professor, Anekant Education Society's College of Pharmacy, Baramati, Maharashtra (MS)-413102⁴Assistant Professor, Dr. V. V. P. F's College of Pharmacy, Vilad Ghat, Ahmednagar Maharashtra (MS)-414111**Article Information**

Received: 07-09-2025

Revised: 25-09-2025

Accepted: 18-10-2025

Published: 22-11-2025

Keywords*Anticancer Activity, Benzimidazole, Breast Cancer, Heterocyclic Compounds, Synthesis, etc.***ABSTRACT**

Since they make up over 80% of pharmaceuticals, heterocyclic molecules are fundamental to drug research. Among natural chemicals, benzoimidazole stands out as a crucial aromatic heterocyclic system that is essential to medicinal chemistry. Beyond its significance in medicine, benzimidazole exhibits adaptability in various fields, including materials science, as well as pharmacological uses that encompass antiviral, antifungal, antioxidant, and anticancer properties. In the present study, 15 derivatives of substituted benzimidazoles were synthesized and evaluated for anticancer activity on the breast cancer cell line MCF-7. Compounds 2a-o was obtained through a multistep synthesis involving the incorporation of substituted benzaldehydes with diamine and sodium bisulfite. The evaluation of anticancer activity by the SRB assay method on the breast cancer cell line MCF-7 shows significant activity. The compounds 2a, 2b, 2c, 2i, 2m, and 2o exhibit greater than 50% cell growth inhibition, and compounds 2d, 2e, and 2h show moderate anticancer potential against the breast cancer cell line MCF-7 by the SRB assay method.

©2025 The authors

This is an Open Access article distributed under the terms of the Creative Commons Attribution (CC BY NC), which permits unrestricted use, distribution, and reproduction in any medium, as long as the original authors and source are cited. No permission is required from the authors or the publishers. (<https://creativecommons.org/licenses/by-nc/4.0/>)

INTRODUCTION:

These days, cancer is the most common deadly illness that is growing as a result of our way of life. Uncontrolled cell growth causes cancer, which is curable if detected early in life. The various internal and external factors that contribute to cancer determine how it is treated. Numerous screening tests are used to detect cancer, and various treatments, including gene therapy, chemotherapy, surgery, radiation therapy, immunotherapy, and more, are now accessible. It is anticipated that 22.2

million more instances of cancer will be diagnosed between now and 2030. [1-3] The benzimidazole scaffold is a functional moiety for the development of novel pharmacological compounds. The benzimidazole nucleus possesses diverse pharmacological activities, including antiulcer, antihypertensive, antiviral, antifungal, anticancer, antihistaminic, antimicrobial, anti-inflammatory, anticonvulsant, antidepressant, antioxidant, radioprotective, and anti-leishmanial activities.[4-8]

MATERIALS AND METHODS:

All chemicals required for the synthesis were brought from Spectrochem Chemicals, Loba Chemicals, S. D. Fine Chemicals, and Sigma Alardrich Chemicals.

Synthesis of substituted benzimidazole derivatives

A series of substituted benzimidazoles 2a-o was synthesized in the laboratory. The purity of the

compound and the completeness of the reaction were monitored by thin-layer chromatography (TLC) using Silica gel 60 F254 (Merck), and the results were identified under UV light. The Gallencamp electric melting point apparatus was used for determining melting points, which were uncorrected. All synthesized compounds were analyzed by KBr disc FT-IR spectroscopy (Jasco Infrared Affinity-1 Spectrophotometer). The ^1H NMR and ^{13}C NMR spectra were recorded in $\text{DMSO-}d_6$ using a Bruker 500 MHz spectrometer (Bruker Biosciences, Billerica, MA, USA), with tetramethylsilane (TMS) used as the internal standard. A Waters Q-TOF Premier mass spectrometer was used to record an HR-MS spectrum, revealing that the molecular ion is $M+1$.

General Procedure

The equimolar amounts (0.1 mmol) of *o*-phenylenediamine and 0.1 mmol of substituted aromatic benzaldehyde were thoroughly mixed in 2 mL of *N,N*-dimethylformamide. Then, 0.1 mmol of sodium bisulfite was added, and the mixture was stirred at 80-90°C for 30 min until the reaction was complete, as indicated by TLC data. The mixture was cooled to room temperature and added

dropwise to 20 ml of water under continuous stirring. The product separated as a solid; it was collected by filtration, washed with warm water, and dried. [9-10]

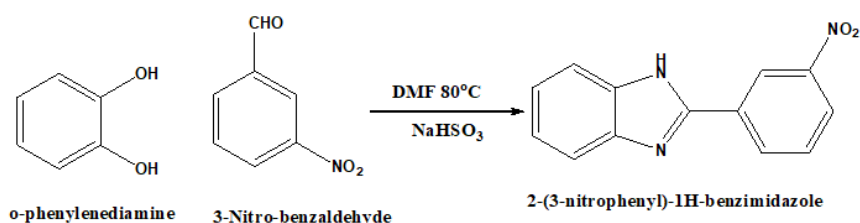
Ethyl [2-(3-nitrophenyl)-1H-benzimidazole-1-yl] acetate

A mixture of equimolar alkaline solution (0.5 mL, 4 N NaOH) and substituted benzimidazole (0.01 mol) in 50 mL of methanol, along with 0.01 mol of ethyl chloroacetate in methanol (20 mL), was heated gently on a boiling water bath for 30 min. The solid thus obtained on cooling was recrystallized from alcohol to give the product.

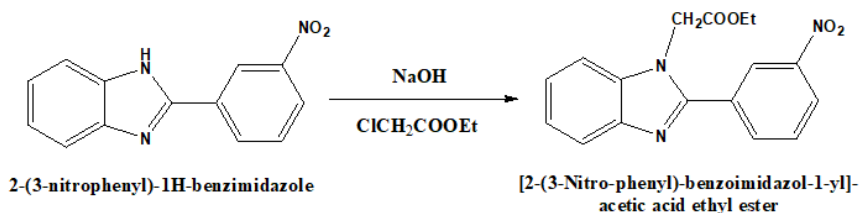
Substituted 2-[2-(3-nitrophenyl)-1H-benzimidazole-1-yl] acetamide analogues

To a solution of ethyl [2-(3-nitrophenyl)-1H-benzimidazole-1-yl]acetate (0.01 mol) dissolved in dry methanol (20 ml), primary amines, substituted hydrazine (1 ml) was added, and the mixture was allowed to stand for reflux for 3-4 hrs. The reaction mixture was cooled, and the solid obtained was filtered and washed with a small quantity of cold methanol to give the product.

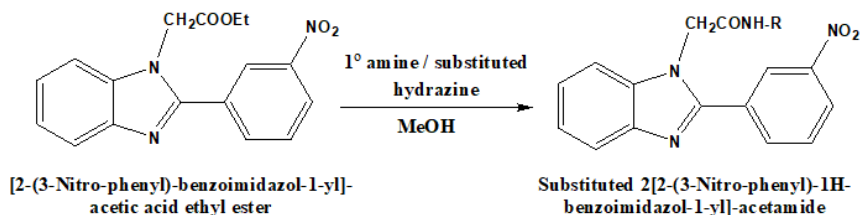
STEP 1:



STEP 2:



STEP 3:



Scheme 1: Synthesis of Benzimidazole Derivatives

EXPERIMENTAL PROCEDURE FOR SULPHORHODAMINE B (SRB) ASSAY:

The cell lines were grown in appropriate medium containing 10% fetal bovine serum and two mM L-glutamine. For the present screening experiment, 5000 cells/well were inoculated into 96-well microtiter plates in 100 μ L. After cell inoculation, the microtiter plates were incubated at 37 $^{\circ}$ C, 5% CO₂, 95% air, and 100% relative humidity for 24 hours prior to the addition of experimental drugs. Experimental drugs were solubilized in an appropriate solvent at 100mg/ml and diluted to 1mg/ml using water and stored frozen prior to use. At the time of drug addition, an aliquot of frozen concentrate (1mg/ml) was thawed and diluted to 100 μ g/ml, 200 μ g/ml, 400 μ g/ml, and 800 μ g/ml with complete medium containing the test article. Aliquots of 10 μ l of these different drug dilutions were added to the appropriate microtiter wells already containing 90 μ l of medium, resulting in the required final drug concentrations, i.e., 10 μ g/ml, 20 μ g/ml, 40 μ g/ml, 80 μ g/ml.

After compound addition, plates were incubated at standard conditions for 48 hours, and the addition of cold TCA terminated the assay. Cells were fixed *in situ* by the gentle addition of 50 μ l of cold 30 % (w/v) TCA (final concentration, 10 % TCA) and incubated for 60 minutes at 4 $^{\circ}$ C. The supernatant was discarded; the plates were washed five times with tap water and air dried. Sulforhodamine B (SRB) solution (50 μ L) at 0.4% (w/v) in 1% acetic acid was added to each well, and the plates were incubated for 20 minutes at room temperature. After staining, the unbound dye was recovered, and the residual dye was removed by washing five times with 1 % acetic acid. The plates were air-dried. The bound stain was subsequently eluted with 10 mM Tris base, and the absorbance was measured on a plate reader at a wavelength of 540 nm with a 690 nm reference wavelength. The percentage growth was calculated on a plate-by-plate basis for test wells relative to control wells. Percent Growth was expressed as the ratio of the average absorbance of the test well to the average absorbance of the control wells * 100. Using the six absorbance measurements [time zero (Tz), control growth (C), and test growth in the presence of drug at the four concentration levels (Ti)], the percentage growth was calculated at each of the drug concentration levels. Growth inhibition of 50 % (GI50) drug concentration resulting in a 50% reduction in the net protein increase (as measured by SRB staining) in control cells during the drug incubation. Values were calculated for each of these three parameters when the level of activity was reached; however, if the effect was not achieved or exceeded, the values for that parameter were expressed as greater than or less than the maximum

or minimum concentration tested. [11-15]

Molecular Docking:

Within this framework, molecular docking has emerged as one of the most used computational methods for repurposing drugs toward potential therapeutic targets. Docking, for instance, may be used in the process of reverse screening, which seeks to recognize new molecular targets for existing ligands on the basis of the structural complementarity between the two. Docking makes it possible to visually analyse databases of authorized pharmaceuticals, natural products, or chemicals that have previously been synthesized into one or more biological targets of interest in a cost-effective amount of time. Docking, as a method for assisting with the many tasks involved in drug development, has undergone similar transformations throughout the course of its history. Docking, in example, was originally conceived and implemented as a technique that could be used on its own; however, in modern practice, it is often utilized in conjunction with other computational strategies within the context of integrated workflows. This makes it possible to get beyond some of the most significant inherent restrictions that are associated with molecular docking, such as the sampling of just a subset of conformations and the use of approximatively scoring systems. In most cases, enhanced prediction performances may be achieved by the use of combination techniques, which also makes it possible to more effectively leverage information coming from a variety of sources. In point of fact, several applications of integrated workflows, such as docking, have been investigated for their potential to aid in the process of drug discovery. In order to further optimization, the derivatives were subjected for binding affinity studies with human angiotensin receptor. The Autodock vina 1.1.2 with PyRx Virtual Screening Tool 0.8 software of the Chimera version 1.10.2 and the Biovia Discovery studio was used to perform molecular docking. The structures of 2-(2-phenyl-1H-benzo[d]imidazol-1-yl)acetic acid derivatives and native ligand were drawn using ChemDraw Ultra 8.0 version and saved in mol file format. The energy minimization was executed by Universal Force Field (UFF) in PyRx software. The crystal structure of the XFEL structure of human Epidermal growth factor receptor (PDB ID: 5WB7) was obtained from the RCSB Protein Data Bank (<https://www.rcsb.org/>). The 3D ribbon view of angiotensin receptor with native ligand is illustrated in Fig. 5.1. The binding mode and binding affinity of native ligand was used to validate the results of designed derivatives. With an exhaustiveness value of 8, the three-dimensional grid box (size_x = 49.1531Ao, size_y = 38.5281Ao, size_z = 42.6578Ao) was modified for molecular docking

simulations. The complete molecular docking approach was carried out in accordance with the methods outlined . [16-22]

RESULTS AND DISCUSSION

PHYSICO-CHEMICAL AND SPECTRAL ANALYSIS OF SYNTHESIZED COMPOUNDS

From scheme 1 fifteen compounds were synthesized. The physicochemical data of the compounds are tabulated in Table 1.

Table 1: The physicochemical data of the synthesized compounds

Code	Molecular Formula	Molecular weight (gm/mol)	M.P. (0C)	% Yield	Rf value
2a	C19H20N2O4	340.37	169-172	0.58	0.58
2b	C17H14Cl2N2O4	381.21	180-182	0.61	0.62
2c	C17H14Cl2N2O3	365.21	195-196	0.64	0.71
2d	C17H15N3O5	341.31	174-176	0.67	0.58
2e	C20H22ClN3O2	371.86	155-157	0.72	0.63
2f	C20H21ClN2O2	356.84	161-163	0.56	0.55
2g	C17H16N2O4	312.31	167-170	0.59	0.58
2h	C17H16N2O5	328.31	171-175	0.54	0.61
2i	C17H15ClN2O4	346.76	180-183	0.69	0.58
2j	C16H11Cl3N2O2	369.62	179-182	0.67	0.59
2k	C16H12Cl2N2O3	351.18	169-174	0.63	0.57
2l	C16H14N2O3	282.29	176-178	0.59	0.56
2m	C16H13ClN2O2	300.73	180-182	0.57	0.54
2n	C15H10ClN3O4	331.71	190-193	0.68	0.53
2o	C15H9Cl2N3O4	366.15	186-189	0.57	0.57

STRUCTURAL ELUCIDATION:

Ethyl 2-(2-(3,4-dihydroxyphenyl)-4,5-dimethyl-1H-benzo[d]imidazol-1-yl)acetate (2a)

MS (m/e): 339.11, 340.01 (m+1), 341.81(m+2).FTIR (cm-1): 3287.5 (-NH str.), 3026.6 (Ar -CH str.), 2960.0 (-CH3 str.), 1498.4 (-C=N str.), 1271.0 (-C-N str.). ¹H-NMR (ppm): 6.89-7.56 (m, Ar-H), 5.42 (s, -OH); 2.47- 2.59 (t, -CH3); 1.48(d, methylene protons).¹³C NMR (CHCl₃-d₆400 MHz) δ ppm:15.56, 17.79, 19.89, 52.16, 62.01, 62.68, 112.56, 114.61, 116.99, 117.45, 123.88, 124.46, 125.31, 125.89, 129.99, 130.73, 137.82, 145.56, 146.89, 152.67, 165.89, 166.34.

Ethyl 2-(4,5-dichloro-2-(3,4-dihydroxyphenyl)-1H-benzo[d]imidazol-1-yl)acetate (2b)

MS (m/e): 380.98, 381.78 (m+1), 383.17 (m+2).FTIR (cm-1): 3384.4 (-NH str.), 3276.3 (Ar -CH str.), 2795.5 (-CH3 str.), 1591.6 (-C=N str.), 1271.0 (-C-N str.). ¹H-NMR (ppm): 6.80-7.45(m, Ar-H), 5.38(s, -OH); 1.39-1.45(t, -CH3) and 2.21(d, methylene protons).¹³C NMR (CHCl₃-d₆400 MHz) δ ppm:15.37, 51.88, 61.76, 115.12, 115.73, 117.31, 122.18, 124.19, 125.34, 126.02, 129.15, 134.21, 140.45, 147.37, 148.08, 154.29, 168.09.

Ethyl 2-(2-(3,4-dichlorophenyl)-4-hydroxy-1H-benzo[d]imidazol-1-yl)acetate (2c)

MS (m/e): 365.39, 366.27 (m+1), 367.89 (m+2). FTIR (cm-1): 3287.5 (-NH str.), 3026.6 (Ar -CH str.), 2851.4 (-CH3 str.), 1621.4 (-C=N str.), 1271.0 (-C-N str.), 693.3, 741.7, 831.2 (aromatic region). ¹H-NMR (ppm): 7.33-7.98(m, Ar-H), 5.35(s, -OH), 4.22(q, of -CH₂); 1.09-1.15(t, -CH₃).¹³C

NMR (CHCl₃-d₆400 MHz) δ ppm:14.47, 50.76, 60.03, 98.82, 102.98, 121.45, 126.31, 128.12, 129.38, 130.06, 132.09, 133.23, 134.53, 147.54, 153.04, 166.76.

Ethyl 2-(4-hydroxy-2-(4-nitrophenyl)-1H-benzo[d]imidazol-1-yl) acetate (2d)

MS (m/e): 340.08, 342.67 (m+2), 344.23 (m+4).FTIR (cm-1): 3287.5 (-NH str.), 3030.3 (Ar -CH str.), 2668.8 (-CH3 str.), 1621.4 (-C=N str.), 1271.0 (-C-N str.), 961.7, 741.7, 827.5 (aromatic region). ¹H-NMR (ppm): 6.88-7.18 (m, Ar-H), 5.35(s, -OH); 4.19- 4.24 (q, -CH₂) 1.41-1.46(t, -CH₃).¹³CNMR (CHCl₃-d₆400 MHz) δ ppm: 15.77, 51.66, 61.76, 98.20, 102.18, 120.71, 123.33, 125.42, 133.28, 134.09, 135.55, 145.67, 145.99, 151.56, 165.69.

Ethyl 2-(5-chloro-2-(4-(dimethylamino)phenyl)-4-methyl-1H-benzo[d]imidazol-1-yl)acetate (2e)

MS: (m/e):372.81, 373.78 (m+1). FTIR (cm-1): 3287.2 (-NH str.), 3030.3 (Ar -CH str.), 2922.2, 2668.8 (-CH3 str.), 1498.4. (-C=N str.), 1271 (-C-N str.), 670.9, 742.7, 823.7.¹H-NMR (ppm): 6.78-7.32 (m, Ar-H), 4.18-4.25 (q, -CH₂), 2.47 (d, dimethylamino proton), 1.41-1.45(t, -CH₃).¹³C NMR (CHCl₃-d₆400 MHz) δ ppm:13.55, 15.68, 41.71, 50.51, 61.02, 112.30, 113.76, 120.12, 124.08, 125.09, 128.03, 129.45, 132.08, 140.02, 153.62, 155.65, 167.98.

Ethyl 2-(5-chloro-2-(3,5-dimethylphenyl)-4-methyl-1H-benzo[d]imidazol-1-yl)acetate (2f)

MS (m/e): 357.34, 358.13 (m+1), 361.98 (m+3).FTIR (cm-1): 3256.45 (-NH str.), 3015.24 (Ar -CH str.); 2865.34 (-CH3 str.), 1578.34 (-C=N

str.), 1265.35 (-C-N str.) 670.9, 742.7, 823.7. ¹H-NMR (ppm): 7.07-7.83 (m, Ar-H), 4.08-4.17 (q, -CH₂) 2.40 (s, -CH₃), 1.30-1.39 (t, -CH₃). ¹³C NMR (CHCl₃-d₆400 MHz) δ ppm: 15.28, 17.13, 23.12, 51.19, 61.11, 113.12, 123.88, 124.17, 128.01, 129.76, 130.31, 131.18, 134.09, 138.61, 139.39, 152.49, 166.63.

Methyl 2-(2-(2,4-dihydroxyphenyl)-4-methyl-1H-benzodjimidazol-1-yl)acetate (2g)

MS (m/e): 314.19, 316.56 (m+2), 320.21 (m+4). FTIR (cm⁻¹): 3324.8 (-NH str.), 3056.4 (Ar -CH str.), 2929.7 (-CH₃ str.), 1520.8 (-C=N str.), 1241.2 (-C-N str.), 823.7, 894.6, 928.1, 689.6. ¹H-NMR (ppm): 6.28-7.82 (m, Ar-H), 5.35(s, -OH); 3.64 (s, -CH₂) 2.36(t, -CH₃). ¹³C NMR (CHCl₃-d₆400 MHz) δ ppm: 16.00, 50.08, 51.76, 105.04, 106.78, 109.02, 110.91, 122.67, 123.98, 125.38, 129.67, 133.88, 138.01, 152.24, 155.78, 159.23, 165.34.

Methyl 2-(2-(3,4-dihydroxyphenyl)-4-methoxy-1H-benzodjimidazol-1-yl)acetate (2h)

MS (m/e): 330.10, 331.99 (m+1), 333.17 (m+3). FTIR (cm⁻¹): 3324.8 (-NH str.), 3060.1 (Ar -CH str.), 2851.4 (-CH₃ str.), 1625.1 (-C=N str.), 1241.2 (-C-N str.), 715.6, 820.0, 928.1. ¹H-NMR (ppm): 7.10-7.55 (m, Ar-H), 5.35(s, -OH); 3.60, 3.88 (q, -CH₃). ¹³C NMR (CHCl₃-d₆400 MHz) δ ppm: 49.87, 51.09, 55.31, 101.45, 109.11, 113.61, 115.62, 120.16, 122.18, 123.81, 132.01, 134.20, 145.13, 146.02, 148.09, 152.12, 164.64.

Methyl 2-(5-chloro-2-(3,4-dihydroxyphenyl)-4-methyl-1H-benzodjimidazol-1-yl)acetate (2i)

MS (m/e): 348.10, 349.02 (m+1), 350.08 (m+3). FTIR (cm⁻¹): 3183.1 (-NH str.), 2926.0 (Ar -CH str.), 2847.7 (-CH₃ str.), 1572.9 (-C=N str.), 1241.2 (-C-N str.), 715.6, 823.7, 928.1, 894.6. ¹H-NMR (ppm): 7.10-7.85 (m, Ar-H), 5.35(s, -OH); 3.70, 3.84 (s, -CH₃). ¹³C NMR (CHCl₃-d₆400 MHz) δ ppm: 16.09, 50.37, 52.10, 113.11, 113.88, 115.82, 123.03, 123.78, 124.01, 124.23, 128.03, 132.10, 139.18, 145.01, 146.71, 153.27, 165.66.

Methyl 2-(4,5-dichloro-2-(3-chlorophenyl)-1H-benzodjimidazol-1-yl)acetate (2j)

MS (m/e): 368.11, 371.78 (m+3). FTIR (cm⁻¹): 3324.8 (-NH str.); 3063.9 (Ar -CH str.); 2847.7 (-CH₃ str.); 1520.8 (-C=N str.); 1285.9 (-C-N str.), 708.2, 820.0, 928.1. ¹H-NMR (ppm): 7.33-8.10 (m, Ar-H), 4.66 (d, methylene protons) 3.84 (t, -CH₃). ¹³C NMR (CHCl₃-d₆400 MHz) δ ppm: 49.68, 50.08, 112.10, 119.67, 123.89, 125.10, 126.66, 127.27, 130.09, 131.72, 133.71, 137.72, 151.19, 164.08.

Methyl 2-(2-(2,4-dichlorophenyl)-5-hydroxy-1H-benzodjimidazol-1-yl)acetate (2k)

MS (m/e): 351.23, 352.78 (m+1), 354.09 (m+3). FTIR (cm⁻¹): 3324.8 (-NH str.); 3056.4 (Ar -CH str.); 2926.0 (-CH₃ str.); 1576.7 (-C=N str.); 1271.0 (-C-N str.), 704.5, 820.0, 890.8, 931.8. ¹H-NMR (ppm): 7.01-8.10 (m, Ar-H), 5.40(s, -OH); 4.08-4.11(q, -CH₂). ¹³C NMR (CHCl₃-d₆400 MHz) δ ppm: 50.04, 52.05, 102.06, 111.01, 113.12, 126.02, 126.41, 129.31, 130.03, 132.56, 135.11, 135.81, 139.67, 151.09, 152.48, 165.41.

2-(2-(4-hydroxyphenyl)-5-methyl-1H-benzodjimidazol-1-yl) acetic acid (2l)

MS (m/e): 282.09, 283.65 (m+1), 285.18 (m+3). FTIR (cm⁻¹): 3324.8 (-NH str.); 2974.4 (Ar -CH str.); 2851.5 (-CH₃ str.); 1625.1 (-C=N str.); 1431.3 (-C-N str.), 864.7, 823.7, 685.8, 898.3. ¹H-NMR (ppm): 7.02-7.49 (m, Ar-H), 5.35(s, -OH); 4.06-4.11(q, -CH₂) 2.37(t, -CH₃). ¹³C NMR (CHCl₃-d₆400 MHz) δ ppm: 20.18, 49.89, 109.42, 110.05, 117.12, 119.45, 123.93, 124.18, 125.77, 131.08, 144.21, 150.03, 165.23.

2-(2-(3-chlorophenyl)-5-methyl-1H-benzodjimidazol-1-yl) acetic acid (2m)

MS (m/e): 302.32, 305.28 (m+3), 306.01 (m+4). FTIR (cm⁻¹): 3285.48 (-NH str.); 3015.45 (Ar -CH str.); 2864.26 (-CH₃ str.); 1590.35 (-C=N str.); 1265.32 (-C-N str.). ¹H-NMR (ppm): 7.29-8.10 (m, Ar-H), 4.06-4.13(q, -CH₂) 2.38(t, -CH₃). ¹³C NMR (CHCl₃-d₆400 MHz) δ ppm: 26.40, 56.02, 115.04, 115.41, 125.34, 126.10, 128.18, 129.12, 130.23, 131.21, 132.00, 134.08, 137.89, 151.57, 172.10.

2-(2-(4-chlorophenyl)-5-nitro-1H-benzodjimidazol-1-yl) acetic acid (2n)

MS (m/e): 332.16, 333.67 (m+1), 336.76 (m+4). FTIR (cm⁻¹): 3245.28 (-NH str.); 3025.65 (Ar -CH str.); 2850.26 (-CH₃ str.); 1585.35 (-C=N str.); 1252.64 (-C-N str.). ¹H-NMR (ppm): 7.02-8.54 (m, Ar-H), 4.06-4.13 (q, -CH₂). ¹³C NMR (CHCl₃-d₆400 MHz) δ ppm: 55.55, 110.04, 112.32, 117.82, 127.01, 127.67, 132.57, 137.38, 138.18, 142.09, 150.03, 171.01.

2-(2-(2,4-dichlorophenyl)-5-nitro-1H-benzodjimidazol-1-yl)acetic acid (2o)

MS (m/e): 367.99, 370.02 (m+1). FTIR (cm⁻¹): 3228.26 (-NH str.); 3010.65 (Ar -CH str.); 2865.30 (-CH₃ str.); 1590.35 (-C=N str.); 1265.38 (-C-N str.). ¹H-NMR (ppm): 7.33-7.81 (m, Ar-H), 3.46-4.11(q, -CH₂). ¹³C NMR (CHCl₃-d₆400 MHz) δ ppm: 54.98, 109.43, 112.05, 117.45, 125.78, 128.18, 129.04, 131.65, 134.06, 134.76, 137.89, 138.02, 142.11, 150.21, 170.32.

EXPERIMENTAL PROCEDURE FOR SULPHORHODAMINE B (SRB) ASSAY:

The anticancer activity of compounds 2a-o was determined by Sulphorhodamine (SRB) assay with MCF-7 Cell line for breast cancer. The anticancer drug Adriamycin was used as the reference standard. Morphological changes of the human breast cancer cell line MCF-7 after treatment. MCF-

7 cell were treated with synthesized compounds (2a-o) for 48 hrs and morphological changes of cell were observed under a transmission electron microscope. MCF-7 cells were also illustrated in Figure 2 and Table 2.

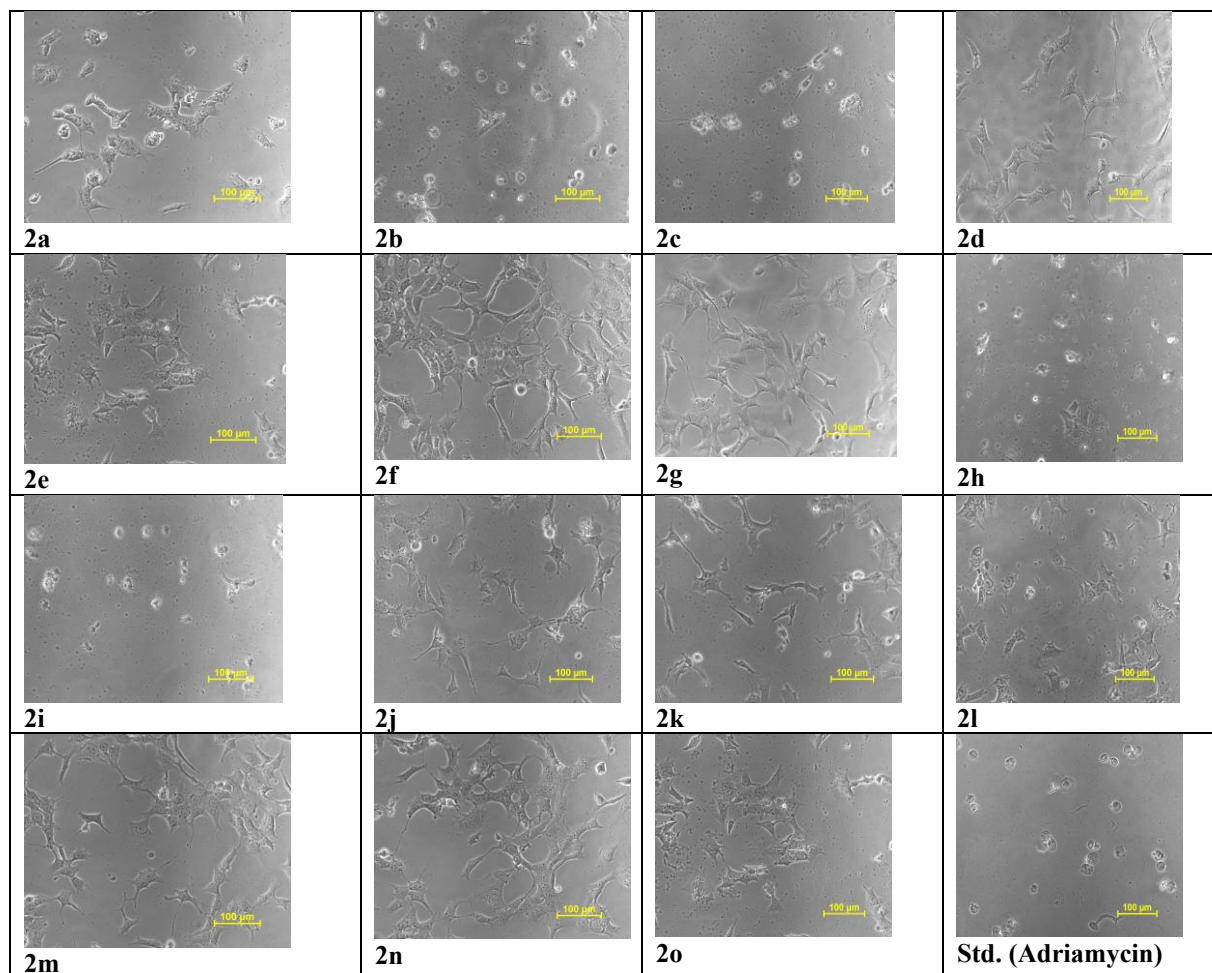


Figure 2: Morphological changes of the human breast cancer cell line MCF-7 after treatment. MCF-7 cell were treated with synthesized compounds (2a-o) for 48 hrs and morphological changes of cell were observed under a transmission electron microscope.

Table 2: Anticancer Activity of synthesized compounds on human breast cancer cell line MCF-7.

Sr. No.	Compound Code	Drug Concentration (µg/ml) GI ₅₀		
		LC ₅₀	TGI	GI ₅₀
1.	2a	NE	>80	49.3
2.	2b	NE	>80	36.2
3.	2c	NE	>80	42.5
4.	2d	NE	>80	58.9
5.	2e	NE	>80	56.7
6.	2f	NE	>80	>80
7.	2g	NE	>80	78.7
8.	2h	NE	>80	54.8
9.	2i	NE	>80	29.6
10.	2j	NE	>80	>80
11.	2k	NE	>80	68.4
12.	2l	NE	>80	63.5
13.	2m	NE	>80	42.2
14.	2n	NE	>80	>80
15.	2o	NE	>80	26.2
16.	Adria	NE	<10	<10

mycin (Standard)				
LC ₅₀ = Concentration of drug causing 50% cell kill GI ₅₀ = Concentration of drug causing 50% inhibition of cell growth TGI = Concentration of drug causing total inhibition of cell growth ADR = Adriamycin, Positive control compound				

MOLECULAR DOCKING

Table 3: Docking Score of synthesized compounds with EGFR Receptor (PDB ID: 5WB7)

Sr. No.	Compound	Docking score
1	2a	-5.085423
2	2b	-4.553250
3	2c	-5.157852
4	2d	-3.780256
5	2e	-3.445888
6	2f	-5.877785
7	2g	-4.665522

8	2h	-4.778589
9	2i	-5.663548
10	2j	-3.556847
11	2k	-4.554635
12	2l	-4.005862

13	2m	-4.785624
14	2n	-2.785484
15	2o	-5.552326
16	Adriamycin (Standard)	-5.125846

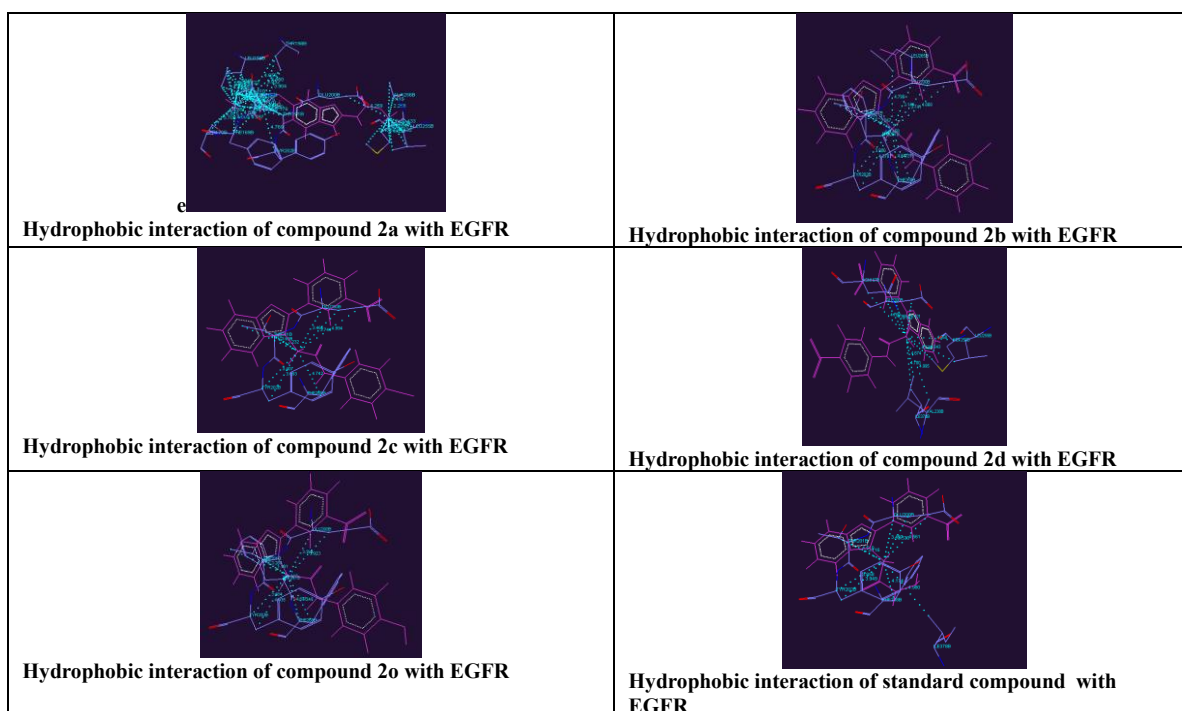


Figure 3: Molecular Docking interactions of synthesized compounds with EGFR Receptor (PDB ID: 5WB7)

CONCLUSION:

In the present study, compounds 2a-o was obtained through a multistep synthesis involving the incorporation of substituted benzaldehydes with diamine and sodium bisulfite. The evaluation of anticancer activity by the SRB assay method on the breast cancer cell line MCF-7 shows significant activity. The evaluation of anticancer activity using the SRB assay method on the breast cancer cell line MCF-7 shows significant activity. The compounds **2a**, **2b**, **2c**, **2i**, **2m**, and **2o** show > 50 % cell growth inhibition, and compounds **2d**, **2e**, and **2h** show moderate anticancer potential. The results obtained from the docking study and biological activity are largely consistent.

ACKNOWLEDGEMENT:

The Author is thankful to Anekant Education Society's College of Pharmacy, Baramati and Shubham University, Bhopal for Providing all the necessary facilities for conducting the research work.

REFERENCES:

- Howlader N, Chen HS, Noone AM, et al. Impact of COVID-19 on 2021 cancer incidence rates and potential rebound from 2020 decline. *J Natl Cancer Inst.* Published online September 24, 2024. doi: 10.1093/jnci/djae180
- Yabroff KR, Wu XC, Negoita S, et al. Association of the COVID-19 pandemic with patterns of statewide cancer services. *J Natl Cancer Inst.* 2022;114(6):907-909. doi: 10.1093/jnci/djab122
- Van den Puttelaar R, Lansdorp-Vogelaar I, Hahn AI, et al. Impact and recovery from COVID-19-related disruptions in colorectal cancer screening and care in the US: a scenario analysis. *Cancer Epidemiol Biomarkers Prev.* 2023;32(1):22-29. doi: 10.1158/1055-9965.EPI-22-0544
- J. Valdez, R. Cedillo, A. Hernandez-Campos, L. Yopez, F. Hernandez-Luis, G. Navarrete-Vazquez, A. Tapia, R. Cortes, M. Hernández and R. Castillo, Synthesis and antiparasitic activity of 1H-benzimidazole derivatives, *Bioorg. Med. Chem. Lett.*, 2002, 12(16), 2221–2224
- F. M. Abdelrazek, M. E. Zaki, S. A. Al-Hussain, B. Farag, A. M. Hebshy, M. S. Abdelfattah, S. M. Hassan, A. F. El-Faragy, L. Iovkova and D. Mross, Facile one-pot synthesis and in silico study of new heterocyclic scaffolds with 4-pyridyl moiety: Mechanistic insights and X-ray crystallographic elucidation, *Heliyon*, 2024, 10(7), e29221
- H. Debus, Ueber die einwirkung des ammoniak auf glyoxal, *Justus Liebigs Ann. Chem.*, 1858, 107(2), 199–208
- G. Satija, B. Sharma, A. Madan, A. Iqbal, M. Shaquiquzzaman, M. Akhter, S. Parvez, M. A. Khan and M. M. Alam, Benzimidazole based derivatives as anticancer agents: Structure activity relationship analysis for various targets, *J. Heterocycl. Chem.*, 2022, 59(1), 22–66
- R. Ranjith, The chemistry and biological significance of imidazole, benzimidazole, benzoxazole, tetrazole and quinazolinone nucleus, *J. Chem. Pharm. Res.*, 2016, 8(5), 505–526
- Tzani MA, Gabriel C, Lykakis IN. Selective Synthesis of Benzimidazoles from o-Phenylenediamine and Aldehydes

- Promoted by Supported Gold Nanoparticles. *Nanomaterials* (Basel). 2020 Dec 1;10(12):2405. doi: 10.3390/nano10122405. PMID: 33271922; PMCID: PMC7760220.
10. Narasimhan B., Sharma D., Kumar P. Benzimidazole: A medicinally important heterocyclic moiety. *Med. Chem. Res.* 2012;21:269–283. doi: 10.1007/s00044-010-9533-9.
 11. Vanicha Vichai and Kanyawim Kirtikara. Sulforhodamine B colorimetric assay for cytotoxicity screening *Nature Protocols* 1: 1112–1116, 2006.
 12. Jyoti Kode, Jeshma Kovvuri, Burri Nagaraju, Shailesh Jadhav, Madan Barkume, Subrata Sen, Nirmal Kumar Kasinathan, Pradip Chaudhari, Bhabani Shankar Mohanty, Jitendra Gour, Dilep Kumar Sigalapalli, C. Ganesh Kumar, Trupti Pradhan, Manisha Banerjee and Ahmed Kamal. Synthesis, biological evaluation and molecular docking analysis of phenstatin based indole linked chalcones as anticancer agents and tubulin polymerization inhibitors. *Bioorganic Chemistry*, 105, 104447, 2020
 13. Faisal Kholiya, Shruti Chatterjee, Gopal Bhojani, Subrata Sen, Madan Barkume, Nirmal Kumar Kasinathan, Jyoti Kode, Ramavatar Meena. Seaweed polysachharide derived bioaldehyde nanocomposite: Potential application in anticancer therapeutics. *Carbohydrate Polymers*. Online published 20.04.2020; Vol 240, July Issue.
 14. Skehan, P.; Storeng, R.; Scudiero, D.; Monks, A.; McMahon, J.; Vistica, D.; Warren, J.T.; Bokesch, H.; Kenney, S.; Boyd, M.R. New colorimetric cytotoxicity assay for anticancer-drug screening. *J Natl Cancer Inst.*, 82: 1107-1112, 1990.
 15. Cava, C.; Castiglioni, I. Integration of Molecular Docking and in Vitro Studies: A Powerful Approach for Drug Discovery in Breast Cancer. *Appl. Sci.* 2020, 10(19), 1–18. <https://doi.org/10.3390/app10196981>.
 16. Stanzione, F.; Giangreco, I.; Cole, J. C. Use of Molecular Docking Computational Tools in Drug Discovery. *Progress in Medicinal Chemistry*, 2021, 60, 273–343. <https://doi.org/10.1016/bs.pmch.2021.01.004>.
 17. Pinzi, L. & Rastelli, G. Molecular docking: Shifting paradigms in drug discovery. *Int. J. Mol. Sci.* 20, 4331 (2019).
 18. Tao, X. et al. Recent developments in molecular docking technology applied in food science: A review. *Int. J. Food Sci. Technol.* 55, 33–45 (2020).
 19. Pramanik, A., Sahoo, R. N., Pradhan, S. K. & Mallick, S. Characterization and molecular docking of kaolin-based cellulosic film for extending ophthalmic drug delivery. *Indian J. Pharm. Sci.* 83(4), 794–807 (2021).
 20. Sahoo, R. N. et al. Interactions between Ibuprofen and Silicified MCC: Characterization, drug release, and modeling approaches. *Acta Chima Slovica* 66(4), 923–933 (2019).
 21. Bissantz, C., Folkers, G. & Rognan, D. Protein-based virtual screening of chemical databases. 1. Evaluation of different docking/scoring combinations. *J. Med. Chem.* 43(25), 4759–4767 (2000).
 22. Tomar, N. R. et al. Molecular docking studies with rabies virus glycoprotein to design viral therapeutics. *Indian J. Pharm. Sci.* 72(4), 486 (2018).